Constitutive modelling approach for evaluating the triggering of flow slides

Constitutive modelling approach for evaluating the triggering of flow slides

Giuseppe Buscarnera[†] and Andrew J. Whittle[††]

[†] Politecnico di Milano – Department of Structural Engineering
Piazza Leonardo da Vinci, 32 – 20132 – Milan (Italy)
[††] Massachusetts Institute of Technology (MIT) – Civil and Environmental Engineering Department
Massachusetts Avenue, 77 – Cambridge (MA) - USA

ABSTRACT

The paper presents a methodology to evaluate flow slide susceptibility in potentially liquefiable sandy slopes. The proposed approach accounts for both contractive and dilative volumetric behaviour during shearing using the MIT-S1 constitutive model. As a result, it is possible to distinguish among different types of undrained response induced by a rapid shear perturbation. The first part of the paper describes the general methodology for infinite slopes, providing an index of stability for incipient static liquefaction in shallow deposits. The methodology accounts for anisotropy due to the initial stress state within the slope and uses simple shear simulations to assess instability conditions as a function of slope angle, stress state and density of the soil. The resulting stability charts define the margin of safety against static liquefaction and the depths likely to be affected by the propagation of an instability. The second part of the paper applies the methodology to the well known series of flow failures in a berm at the Nerlerk site. The MIT-S1 model is calibrated using published data on Nerlerk sands and in situ CPT data. The analyses show that in situ slope angles α=10°-13° are less than the critical slope angle needed for incipient instability. The analyses show that liquefaction and flow failures are likely for small perturbations in shear stresses that could be generated by rapid deposition of hydraulic fill.

KEY WORDS: Static liquefaction, slope stability, flow slide, constitutive modelling, soil instability.

INTRODUCTION

Landslides and slope failures are widely recognized as an important class of natural hazards that has relevance at a range of scales, from the design of earthworks to the management of land use in densely populated areas. The wide distribution of these phenomena represents a continuing challenge for the geotechnical community to develop appropriate tools of analysis, explain complex failure mechanisms, evaluate and mitigate current hazards and define reliable design criteria. Within the general class of slope failures, runaway instabilities associated with flow slides in cohesionless soils are particularly impressive phenomena that involve several unanswered research questions. The geotechnical literature reports several case histories of large submarine flow slides [Koppejan et al., 1948; Terzaghi, 1957; Andersen and Bjerrum, 1968]. Flow slides in submerged artificial sandy slopes can also represent a major threat in coastal environments, where deposition, dredging and excavation can produce rapid shear perturbations in the soil mass [Sladen et al., 1985-b; Hight et al., 1999; Yoshimine et al. 1999].

One of the first interpretations of these slope failures was due to Terzaghi (1957). In order to characterize the observed phenomenon, Terzaghi introduced the term spontaneous liquefaction, relating this typology of slope instability to the metastable state of the deposits involved. Most of the attempts to define quantitatively the triggering conditions for a flow slide have been based either on semi-empirical frameworks relying on the concept of steady state of deformation [Castro, 1969; Poulos, 1981; Poulos et al., 1985] or on the definition of instability boundaries in effective stress space [Sladen et al., 1985-a; Lade 1992]. However, none of these approaches is sufficiently general for a practical implementation into triggering analyses.

Experimental observations and analyses of case studies have shown that many different factors can affect both the necessary perturbation to induce an instability and the post-failure behaviour (e.g., drainage and test control conditions, relative density and stress level, anisotropy etc.). Recent advances in soil constitutive modelling can provide powerful tools to shed light on this complex issue. One of the first and most interesting modelling approaches to address the problem of flow slide triggering using a thorough description of soil behaviour was proposed by di Prisco et al. (1995), with particular reference to the simple case of an infinite slope.

This paper presents a methodology to evaluate flow slide susceptibility in a potentially liquefiable sandy slope based on the original idea suggested by di Prisco et al. (1995), but tries to link more directly the model predictions to the framework of critical state for cohesionless materials and to in situ observations. The key contribution is the ability to predict transitions between contractive and dilative volumetric behaviour upon shearing. As a result, the approach is able to distinguish among different types of sand response induced by an undrained perturbation (complete liquefaction, partial liquefaction, etc.), which is an essential aspect to define the expected post-failure behaviour of a sliding mass. The MIT-S1 model (Pestana and Whittle, 1999) is used for this purpose. The model accounts for some of the most relevant factors affecting the undrained response of sands (e.g., density dependence, pressure dependence, initial and evolving anisotropy etc.). Here it is combined with an appropriate stability criterion for shallow slopes. In this way, the influence of slope angle, stress state and density of the deposit are investigated synthetically, evaluating the magnitude of the stress perturbation necessary to trigger liquefaction. This is done by producing stability charts for any depth in the slope that identify the margin of safety from static liquefaction and the location of the soil masses likely to be affected by the propagation of an instability.

Finally, the approach is applied to a well known series of flow failures at the Nerlerk berm (Sladen et al., 1985-b), in which sand liquefaction is likely to have played a relevant role. Experimental data relative to both laboratory tests and CPT in situ tests available in the literature are used and interpreted, in an attempt of providing a consistent mechanical interpretation of the phenomenon.

REVIEW OF DEVELOPMENTS IN TRIGGERING OF FLOW SLIDES

Several authors in the past addressed the problem of flow slides induced by static liquefaction. The first approaches were essentially focused on the experimental definition of liquefaction conditions under undrained loading [Castro, 1969] and the introduction of the steady state strength in classical limit equilibrium analyses [Poulos, 1981; Poulos et al., 1985]. Although the steady state strength can be used to evaluate soil liquefaction potential at very large strains, it does not address the initial triggering conditions for a flow failure. In addition, there are circumstances in which the use of the steady state strength can be misleading. Liquefaction instabilities can also be triggered in soils experiencing dilation at large strains, provided that the excess pore pressures induced prior to shearing is large enough to induce a structural soil collapse (partial liquefaction). In this case a proper instability is still possible, but with a marked change in the post-failure response of the slope [Beezuijen and Mastbergen, 1989].

A more general understanding of the flow slide triggering was achieved when it was fully recognized that potential instability conditions can be attained even when the soil is loaded along drained stress paths, provided that certain shear stress levels were achieved after drained loading. This new perspective led to interpretative frameworks based on the definition of instability boundaries in the effective stress space. Important examples of theories of this kind are the collapse surface concept [Sladen et al., 1985-a] and the instability line concept [Lade, 1992], as shown in Fig. 1. These loci in the effective stress space represent a limit of stability under undrained conditions, therefore instability can be initiated when the stress path reaches such loci during either drained or undrained shearing. However, the stress state is not bounded to lie within the limits described by these instability boundaries. Under drained loading the state of stress can cross the boundary without experiencing any collapse, but spontaneous collapse can occur if undrained shearing conditions prevail.

Although these theories favor a relevant improvement in recognizing static liquefaction as a proper soil instability phenomenon, they do not constitute a general interpretation framework. Their development was in fact based almost exclusively on experimental observations derived from triaxial testing, and in most cases the evaluation of the deviatoric stresses triggering liquefaction was estimated for the unlikely conditions of an initial isotropic state of stress. This disregards the influence of different static and kinematic boundary conditions (e.g. plane strain, simple shear conditions etc.), and the influence of the initial anisotropy within the slope. As a result, the adoption of instability parameters estimated from undrained triaxial shear tests is ad hoc and is not predictive for evaluating flow slide triggering under field boundary conditions.

More refined predictive frameworks based on comprehensive constitutive models have been proposed in the literature (Nova, 1989, 1994; Imposimato and Nova 1998; Borja, 2006). The goal of these contributions was to apply the theory of material instability to static liquefaction, providing a mechanical explanation for the phenomenon. Further generalizations of these approaches have been recently developed, disclosing the importance of the current state of stress and density on the liquefaction potential (Andrade, 2009; Buscarnera and Whittle, 2011) and showing practical applications of the theory to finite element analyses (Ellison and Andrade, 2009; Pinheiro and Wan, 2010).

One of the first approaches to consider these notions for the triggering analyses of flow slides was that suggested by di Prisco et al. (1995). In order to study the onset of a flow slide, the authors considered the geometry of an infinite slope and modelled sand behaviour through simple shear simulations. This approach was able to combin the accuracy given by advanced constitutive models with a reduced cost of analysis, and similar approximations to address slope behaviour have been used more recently by other authors to study the onset of subaqueous slides in low permeability clays under cyclic loading (Pestana et al,. 2000; Biscontin et al., 2004) or the tsunamigenic triggering of a shallow underwater slide through energy principles (Puzrin et al., 2004).

The kinematic constraints for the infinite slope geometry (Fig. 2-a) impose plane strain conditions, implying that the out-of-plane strain rate components must be zero (i.e., $\dot{\varepsilon}_{\chi} = \dot{\gamma}_{\chi\xi} = \dot{\gamma}_{\chi\eta} = 0$). The assumption of infinite slope also constrains the extensional strain component parallel to the slope, $\dot{\varepsilon}_{\eta} = 0$. Finally, if undrained shearing occurs, the isochoric constraint implies a zero value for the strain component normal to the slope, $\dot{\varepsilon}_{\xi} = 0$. As a result, the only strain contribution governing the undrained behaviour of an infinite slope is the shear strain $\dot{\gamma}_{\xi\eta}$ (i.e., the material points at any depth are subject to undrained simple shear mode). Therefore, provided that suitable initial test conditions are defined in simple shear test simulations, a description for the undrained response of the slope can be predicted by material point analyses.

Following these assumptions, di Prisco et al. (1995) described the response of any point in the slope by performing simple shear test simulations, with the initial state corresponding to equilibrium in the slope. Fig. 2b summarizes typical charts of shear perturbations obtained through undrained simple shear simulations. The chart shows the shear stress increment, $\Delta\tau$, necessary to trigger a flow slide as a function of the slope angle. Given the conventional assumption that stress-strain-strength properties can be normalized with respect to the mean effective stress, there is almost no variation of liquefaction susceptibility within the soil mass. As a result, a single normalized chart can represent triggering conditions at all depths within the slope. It is evident that spontaneous flow will occur for slopes having inclinations greater that the angle of spontaneous liquefaction α_{SL}. In other words, slopes with inclinations greater than α_{SL} can suffer a runaway instability even if an infinitesimal triggering perturbation is applied to the slope. This result provides a theoretical basis consistent with Terzaghi's notions of spontaneous liquefaction and incipient instability.

These simplifications imply that slope instability can be fully defined by a single stability chart. As a consequence, the calculation of charts similar to Figure 2-b requires a procedure for depth-averaged undrained shear properties. This is clearly an approximation for real granular materials whose properties depend on stress level and density, and are not adequately described using averaged parameters.

The following sections present a more refined modelling approach that tries to overcome these limitations and describes more realistically triggering conditions for infinite slopes. The goal is to provide a framework that can predict liquefaction susceptibility based on in situ and laboratory data.

MODELLING APPROACH FOR FLOW SLIDE TRIGGERING

The modelling framework presented in this paper is based on the MIT-S1 constitutive model [Pestana and Whittle 1999]. MIT-S1 is a model developed to predict the rate-independent anisotropic behaviour for a broad range of soils (uncemented sands, clays and silts). The model describes the stress-strain-strength properties of cohesionless sands that are deposited at different initial formation densities as functions of both the stress state and current density (void ratio), using a single set of model parameters, i.e. it accounts for both barotropic and pycnotropic effects. Table I summarizes the model parameters which will be used hereafter. A complete description of both model formulation and material parameters is available in Pestana and Whittle (1999).

The current analyses assume that flow slide triggering conditions in infinite slopes can be evaluated by considering the stress-strain properties in an undrained simple shear mode of shearing at a given depth. The initial stress state at the depth of interest is the outcome of complex deposition processes which could be by themselves the subject of separate investigations (di Prisco et al. 1995; Pestana and Whittle, 1995). For the sake of simplicity, the initial stress state can be approximated by calculating $\sigma'_{\xi 0}$ and $\tau_{\xi\eta 0}$ based on equilibrium (as shown in Fig. 2-a) and assuming $\sigma'_{\eta 0} = K_0 \sigma'_{\xi 0}$. This assumption is adequate for low slope angles (Lade, 1993), and it will be adopted hereafter, restricting the analyses to gentle slopes ($\alpha \leq 15°$). The MIT-S1 model also requires the definition of initial directions of material anisotropy. These are introduced through a tensorial internal variable, $\mathbf{b}$, that governs the orientation of the yield surface and evolves as a result of mixed isotropic-kinematic hardening rules. The current analyses assume that the initial stress state coincides with the tip of the yield surface (consistent with prior applications of the model for K_0-consolidation).

Fig. 3 illustrates MIT-S1 simulations of undrained simple shear response at the same level of initial vertical effective stress but with different magnitudes of initial shear stresses τ (representing different slope angles). The simulations have been performed using the model calibration for a reference material (Toyoura sand; see Table I, after Pestana et al., 2002), with vertical stress σ'_{v0}=150 kPa and e=0.93. The results show how the initial state of stress significantly affects the magnitude of the shear perturbation required to induce instability ($\Delta\tau_1$ vs $\Delta\tau_2$). The onset of a mechanical instability coincides with the peak in the shear stress, that is readily apparent from the stress-strain response pictured in Fig. 3-b. Consistent predictions of this circumstance can be obtained from the mathematical notion of controllability (Nova, 1994), according to which any instability mode under mixed stress-strain control is associated with the singularity of the constitutive matrix governing the incremental response. In particular, it can be proved that for elastoplastic strain-hardening models controllability conditions can be evaluated from a critical value of the hardening modulus, H (Klisinski et al., 1992; Buscarnera et al., 2011). For undrained simple shear conditions the critical hardening modulus must be evaluated in accordance with the kinematic constraints outlined in the previous section, and is given by:

$$H_{LSS} = H_C + \frac{\partial f}{\partial \tau_{\xi\eta}} G \frac{\partial g}{\partial \tau_{\xi\eta}} \tag{1}$$

where $\tau_{\xi\eta}$ is the shear stress acting along the slope direction, G is the elastic shear modulus, f the yield surface and g the plastic potential (di Prisco and Nova, 1994). The term H_C in Eq. (1) is the critical hardening modulus for pure strain control than can be expressed in matrix notation as:

$$H_C = -\frac{\widetilde{\partial f}}{\partial \boldsymbol{\sigma}} \mathbf{D}^{\mathbf{e}} \frac{\partial g}{\partial \boldsymbol{\sigma}} \tag{2}$$

where $\mathbf{D}^{\mathbf{e}}$ is the elastic constitutive stiffness matrix and the tilde indicates a transposed vector (Maier and Hueckel, 1979).

The assessment of stability conditions for infinite slopes is then straightforward, and can be conducted by adapting to undrained simple shear conditions the procedure outlined by Buscarnera and Whittle (2011). Starting from Eq. (1), a stability index for undrained simple shear loading can be defined as:

$$\Lambda_{LSS} = H - H_{LSS} \tag{3}$$

In particular, a stable incremental undrained response is predicted for a positive stability index $(\Lambda_{LSS} > 0)$, while a non positive value for Λ_{LSS} marks the conditions necessary for incipient instability. As a result, the initiation of static liquefaction is predicted when the stability index given by Eq. (2) vanishes $(\Lambda_{LSS} = 0)$, as shown in Fig. 3-c.

If the same type of simulation is performed for a range of slope angles, it is possible to evaluate the influence of the slope inclination on the susceptibility to liquefaction instability. Fig. 4 presents further results showing the undrained stress paths at constant normal stress and variable in-situ shear stress $\tau = \sigma'_V \tan\alpha$. These simulations are then used to define the triggering relationship between $\Delta\tau$ and the slope angle α, with triggering shear stresses identified by using the condition $\Lambda_{LSS} = 0$. The progressive approach towards a less stable condition with increasing slope angle is reflected by the reduction in both the triggering shear perturbation and the stability index prior to shearing (Fig. 4-b).

As is well known, the undrained behaviour of sands is significantly influenced by changes in the effective stress and density (Ishihara, 1993). For example, even very loose sands can exhibit a tendency to dilate at low effective stress levels, but will collapse for undrained shearing at high levels of effective stress. Hence, the prediction of liquefaction potential requires a constitutive framework that can simulate realistically the stress-strain properties as functions of stress level and density.

Fig. 5 and 6 illustrate MIT-S1 predictions of the undrained simple shear behaviour for Toyoura sand. The figures show how the stability index Λ_{LSS} makes it possible to differentiate between inception of liquefaction ($\Lambda_{LSS}=0$ and $\dot{\Lambda}_{LSS}<0$), quasi-steady state conditions ($\Lambda_{LSS}=0$ and $\dot{\Lambda}_{LSS}>0$) and critical state at large shear strains ($\Lambda_{LSS}=0$ and $\dot{\Lambda}_{LSS}=0$). In Fig. 5 the in situ pre-shear void ratio varies from 0.87 to 0.94, and the model predicts a sharp transition from a stable behaviour (e_0=0.87) to complete collapse (e_0=0.94). In Fig. 6, post-peak instabilities in the stress-strain behaviour at σ'_{Vc}=100 and 200 kPa are followed by metastable conditions and tendency to dilate at large strains, as illustrated by typical laboratory measurements reported by others (Shibuya, 1985). In the following, these two different types of undrained response will be referred to as *partial liquefaction* and *complete liquefaction*, respectively. According to this terminology, partial liquefaction indicates an undrained response in which the shear stress at large strains is higher than the initial in situ shear stress τ_0, while complete liquefaction addresses an undrained response in which the post-peak shear stress is lower than τ_0 (no recovery of stability at large shear strains).

The outcome of pycnotropic and barotropic effects on undrained sand response is that the perturbation shear stress ratio $\Delta\tau(\alpha,z)/\sigma'_{Vc}$ associated with the initiation of liquefaction is not only a function of the slope angle but must be evaluated at the effective stress and density states at the depth of interest. Fig. 7 gives a qualitative example of the triggering conditions, based on simulations with Toyoura sand as a reference material. In the first series (Fig. 7-a) the effect of several possible initial densities has been considered, keeping constant the initial level of mean effective stress. In contrast, in the second series (Fig- 7-b) considers different pressure levels at constant void ratio.

Once stability charts expressing the shear resistance potential $\Delta\tau(\alpha, z)/\sigma'_{Vc}$ have been obtained, it is possible to define the variation in the triggering perturbation along the profile of a given infinite slope. The transition from liquefiable to non liquefiable response illustrated in Figs. 5-6 is crucial to identify the sand layers that are vulnerable to the propagation of an instability. To achieve this type of prediction, the calibration of model parameters has to be related to the in situ density profile for the specific problem at hand. These capabilities are illustrated through a case study in the following section.

RE-ANALYSIS OF FLOW INSTABILITIES AT THE NERLERK BERM

The Nerlerk berm case history refers to an impressive series of slope failures that took place in 1983 during construction of an artificial island in the Canadian Beaufort Sea. These slope instabilities occurred within a hydraulically placed sand (from a local borrow source). Details on the construction methods, equipment and materials are given by Mitchell (1984). Based on detailed studies of the slide morphology, Sladen et al. (1985-b) classified the slope instabilities as flow slides.

The case of the Nerlerk berm failures represents one of the best documented examples of slope failures in which static liquefaction is considered to have played a relevant role. The underlying causes of the slides have attracted an intense scientific discussion, since the first attempts to back-analyse the phenomenon [Sladen et al., 1985-b; Been et al., 1987; Sladen et al. 1987]. Two main lines of thought were developed. The first considered static liquefaction as the most plausible cause of the flow failure, while the second focused on the role of a possible shear failure involving the seabed soft clay.

Many authors tried to back-analyse Nerlerk slides using a variety of different methodologies, including (i) limit equilibrium analyses to investigate the type of failure mechanism (Rogers et al., 1991), (ii) modified versions of the classical critical state framework for sands (Konrad, 1991), (iii) the use of the notion of incipient instability (Lade 1993) and also (iv) non-linear finite element analyses of the entire berm as a boundary value problem (Hicks and Boughrarou, 1998). Hicks and Boughrarou (1998) present a detailed review of the previous works.

This paper uses the MIT-S1 model to investigate potential static liquefaction mechanisms in the Nerlek berm. The proposed methodology is hereafter applied assuming that the local behaviour of the sides of the berm can be studied through the scheme of infinite slope. Of course, this choice represents an important simplification of the real geometry. However, it is an assumption that enables an immediate evaluation of possible incipient instability within the fill and the type of expected undrained response. Although this type of analysis is conceptually similar to earlier studies based on the notion of incipient instability (Lade, 1993), the current approach relies on the predictions of a constitutive model that are calibrated to site specific properties of the Nerlerk sands.

Calibration of MIT-S1 for Nerlerk Sand

The calibration of the MIT-S1 model for the prediction of instabilities in the Nerlerk berm has required a number of approximations. Although Nerlerk sand has been extensively studied through laboratory tests, there are no published data regarding the 1-D compression behaviour. As a consequence, some model parameters (Table I) have been selected making reference to another Arctic region sand, Erksak. Erksak sand (Been and Jefferies, 1991; Jefferies, 1993) is a clean quartzitic granular material (0.7 % fines content), having D_{50}=330 mm and C_u=1.8. The Nerlerk sand has similar mineralogy and particle size characteristics, with D_{50}=280 mm and C_u=2.0, but with in situ non plastic fines content that ranges from 2% to 15%. Laboratory studies on Nerlerk sands (Sladen et al. 1985-a) have focused on the shear behaviour of specimens with fines contents 0%, 2% and 12%. Additional data on these sands, and a comparison of the grain size distributions of Erksak sand and Nerlerk sands at different fines content are reported in Fig. 8. The following paragraphs summarize the procedure used to calibrate MIT-S1 material parameters for Nerlerk sand with 2% and 12% of fines contents (selected variables are listed in Table I).

Input parameters describing the compression behaviour (ρ_c, p'_{ref}/p_a and θ in Table I) are obtained by fitting low pressure data for Erksak sand (from Jefferies and Been, 1993). This is accomplished using the approximate approach proposed by Pestana and Whittle (1995). Fig. 9 shows the resulting compression behaviour and the Limiting Compression Curve (LCC) that defines high pressure behaviour in the model. The same model parameters are used for Nerlerk sand with 2% and 12% fines, with the exception of θ and p'_{ref}/p_a, that have been estimated by means of empirical correlations (Pestana and Whittle, 1995).

Fig. 10 reports the critical states (CSL) for Erksak sand and Nerlerk sands (2% and 12% fines content). There is considerable judgment involved in the interpretation of the CSL data presented by Sladen et al. (1985-a). The data are fitted using an analytical expression for the CSL that is defined using three model input parameters (ϕ_{mr}, m and p; Table I), as proposed by Pestana et al. (2005). The results show significant differences in the CSL for all the sands and also in the corresponding model input parameters (Table I).

Fig. 11 compares the computed and measured effective stress paths and shows stress-strain behaviour for Nerlerk 2% in undrained triaxial compression shear tests. These data have been used to define some of the remaining model parameters, notably ω_s and ψ (Table I). Fig. 12 confirms that the selected parameters are able to describe reasonably also the drained shear behaviour. Fig. 13 shows similar comparisons of undrained behaviour for Nerlerk-12%. The model captures first order features in the measured behaviour but underestimates the peak shear strength mobilized in these tests.

In situ states and stability charts

In order to apply the MIT-S1 model for the Nerlerk berms it is necessary: a) to define the in situ initial void ratios along the slope profile and b) to evaluate the *stability charts* of the Nerlerk berm for several depths within the slope.

The first step is largely dependent on a reliable interpretation of the available in situ tests. Several CPT tests were performed on the hydraulic fills at Nerlerk, with the aim of extimating the in situ density. The interpretation of these CPT tests has always represented a matter of debate in prior studies of the Nerlerk berm (e.g., Been et al., 1987; Sladen et al., 1987).

It is clear that the choice of a specific interpretation method for CPT test results will affect the estimation of relative density (and, in turn, the model predictions). This uncertainty is probably unavoidable in any method of interpretation.

The current analyses assume that relative density can be estimated using the empirical correlation proposed by Baldi et al. (1982). Fig. 14-a shows that D_r ranges from 30 to 55 %. This approach makes no distinction on the influence of fines content. Fig. 14-b shows the distribution of these initial states relative to the CSL of Nerlerk-12%.

Fig. 15 shows the computed instability curves $\Delta\tau(\alpha,z)/\gamma' z$ at selected depths for infinite slopes in Nerlerk sand with 12% fines content. The results show that the magnitude of the shear perturbation needed to cause instability can be significantly affected by the specific depth within the slope profile.

This result defines the initial stability state of the Nerlerk berm slopes in a proper mechanical sense, providing a prediction of the critical geometry for incipient instability. The Nerlerk berm was constructed at slope angles in the range α =10°-13° and, hence, required additional shear stress to trigger flow failures. In other locations where steeper slopes were recorded, only very small perturbations in shear stress could have triggered failure.

Fig. 16 shows the undrained effective stress paths predicted by MIT-S1 for the same depths investigated in Fig. 15, and for a slope angle $\alpha = 13°$. These results show stable (i.e., potentially dilative) behaviour at z =1 m, partial liquefaction at z =3 m, 8 m (i.e., large strain strength is larger than the initial shear stress) and complete liquefaction at z =5 m, 10 m and 13 m. These results provide predictions of the depths where flow slides are most likely to be triggered. In this case, two different zones in the range z = 5 - 8 m or $z \geq 10$ m are more susceptible to static liquefaction. This result is consistent with what was reported on the basis of bathymetric surveys by Sladen et al. (1985-b), which stated that “the depth of the failed mass varied between 5 and 12 m and the prefailure slope gradients were typically between 10°-12°”.

Fig. 17-a and 17-b illustrate the depth profile of the triggering shear stress for liquefaction based on the stability curves presented in Fig. 15 for slopes having α =10° and 13°, respectively. The results are compared with those that would be obtained for depth-averaged assessment (in this case based on MIT-S1 simulation at z = 8 m and e_0 = 0.73). This average could represent the optimal calibration of a simpler model where the effects of confining pressure and density are not considered. From the picture it is evident that such an averaging procedure can overestimate the liquefaction resistance in some parts of the slope and is not able to distinguish important differences in undrained shear behaviour that make the slope vulnerable to flow failure.

It is clear from Fig. 17 that an undrained perturbation of the shear stress was necessary to trigger flow slides in the Nerlerk berm. A possible source for this stress perturbation could be associated with the rapid deposition of sand at the top of the slope. Assuming uniform filling along the infinite slope, the shear stress perturbation is given by

$$\Delta\tau = \gamma_{SAT} \Delta h \sin\alpha \tag{4}$$

where Δh is the thickness of the deposited sand layer and γ_{SAT} is its total unit weight (here assumed to be equal to 19.4 kN/m^3).

From the above equation and from the limit shear stress given by Fig. 17 it is possible to obtain an estimate of the critical values of additional surcharge required to trigger liquefaction for rapid filling. According to this analysis, failure for a slope with α =10° will be triggered for a rapid fill with Δh = 0.52 - 0.76 m, reducing to Δh = 0.25 - 0.37 m at α =13°.

Discussion

The current analysis of the Nerlerk Berm slides has focused on the possible role played by static liquefaction in the failure mechanism and on the conditions necessary to trigger instability. The quantitative results are clearly related to the assumptions regarding the in situ density of the hydraulic fill and the hypothesis that a rapid deposition during construction could have produced undrained shear perturbations sufficient to trigger instability. While neither of these assumptions is validated by this work, the main purpose is to verify the possible role of liquefaction instability in the triggering of flow slides. Our results, obtained using a site specific calibration of the MIT-S1 model with established empirical correlations for relative density from CPT tests, show that static liquefaction is likely to have played a relevant role in the failure mechanism.

This conclusion is consistent with earlier findings (Sladen et al. 1985-b; Lade 1993). The current analysis provide a more detailed predictive framework that shows critical zones of flow failure may have been located in the range in the range $z = 5 \div 8$ m or $z \geq 10$ m.

The Nerlerk berm slopes were likely not in an incipient unstable state, and an undrained triggering perturbation was a necessary condition for a flow failure. A central point of possible future investigation would therefore have to be focused on the likelihood of temporary undrained conditions during construction.

Although many additional aspects could have been considered in this re-analysis of the Nerlerk slides (e.g., the variability of the in situ density, the role of the fines content and its spatial distribution, the rate of sand deposition, etc.), the present approach captures most of the first order features affecting the liquefaction potential and is able to link in a fairly simple way model predictions at material point level to the in situ response observed at the Nerlerk site.

CONCLUSIONS

This paper presents a framework for evaluating the triggering of flow slides in infinite slopes by modelling the undrained shear behaviour using the anisotropic MIT-S1 model. Stability charts are derived from simulations of undrained simple shear behaviour at a series of material points.

The current approach follows the same kinematic assumptions previously used by di Prisco et al. (1995), but introduces predictive capabilities for simulating instability as a function of the in situ stress and density within the slope. The selected soil model (MIT-S1 model), in fact, is able to simulate realistic transitions in the contractive/dilative response of sands.

Thus, a more complete description of sand behaviour is a key issue in predicting not only the shear perturbations able to induce instability, but also the location within the soil masses and the potential for propagation of a flow failure (static liquefaction). In practice the model needs to be calibrated for the site specific properties of the soil, and requires reliable data on in situ density in order to make predictions of liquefaction potential.

The proposed methodology has been applied to the well known case of slope failures in the Nerlerk berm. A general picture of the distribution of liquefaction susceptibility on the Nerlerk slope profile has been obtained. The analysis are based on the calibration of model input parameters based on published laboratory tests results and empirical correlations for D_r based on CPT data. The results show that there are two zones within the slope that are vulnerable to flow failure (complete liquefaction). Although some sections of the berm slope were oversteepened, most were deposited with α=10°-13°. For these slope angles, the current analyses show that instability can be triggered by rapid deposition of 0.2-0.5 m of hydraulic fill. Thus, static liquefaction is likely to have contributed to the observed failures, confirming earlier hypothesis by Sladen et al. (1985-b).

The current analysis offers a simple, consistent and complete mechanical framework for interpreting and predicting the triggering of flow slides in sands that can be easily applied to other similar engineering cases.

ACKNOWLEDGMENTS

The first author gratefully acknowledges the Rocca Fellowship program, that provided support for his research studies at MIT. The authors are also grateful to Professor Roberto Nova for the useful suggestions during the editing of the manuscript and to Professor Michael Hicks for his assistance in providing laboratory data for the Nerlerk sands.

References

[1] Andresen A,. Bjerrum L. (1968). Slides in subaqueous slopes in sand and silt. *NGI Publication* N. 81, 1-9.

[2] Andrade, J.E. (2009). A predictive framework for static liquefaction. *Géotechnique*, 59: 673-682.

[3] Baldi G., Bellotti R., Ghionna V., Jamiolkowski M., Pasqualini E. (1982). Design parameters for sands from CPT. *Proceedings of the Second European Symposium on Penetration Testing*, ESOPT 11, Amsterdam, Holland, pp. 425-432.

[4] Been, K., Conlin, B. H., Crooks, J. H. A., Fitzpatrick, S. W., Jefferies, M. G., Rogers, B. T., Shinde, S. (1987). Back analysis of the Nerlerk berm liquefaction slides: Discussion. *Can. Geotech. J.*, 24, 170-179.

[5] Been K., Jefferies M.G., Hachey J. (1991). The critical state of sand. *Géotechnique*, 41, 365-381.

[6] Beezuijen A., Mastbergen D.R. (1989). Liquefaction of a sand body constructed by means of hydraulic fill. *Proceeding 12th International Conference on Soil Mechanics and Foundation Engineering*, Rio de Janeiro, Brazil. A.A. Balkema, Rotterdam, vol. 2, pp. 891-894.

[7] Biscontin, G., Pestana, J.M., Nadim, F. (2004). Seismic triggering of submarine slides in soft cohesive soil deposits. *Marine Geology*; 203; 341-354.

[8] Borja, R. I. (2006). Condition for liquefaction instability in fluid-saturated granular soils. *Acta Geotech.* 1, No. 4, 211–224, 2006.

[9] Buscarnera G., Dattola G., di Prisco, C. (2011). Controllability, uniqueness and existence of the incremental response: a mathematical criterion for elastoplastic constitutive laws. International Journal of Solids and Structure, Volume 48, Issue 13, 15 June 2011, Pages 1867-1878.

[10] Buscarnera, G., Whittle, A.J. (2011). Model prediction of static liquefaction: the influence of the initial state on potential instabilities. Submitted for publication to *J. Geotech. Geoenviron. Eng. ASCE.*

[11] Castro, G. (1969). Liquefaction of sands, Harvard Soil Mechanics Series, No.81, Pierce Hall.

[12] di Prisco, C., Nova, R. (1994). Stability problems related to static liquefaction of loose sand, in "Localisation and Bifurcation Theory for Soils and Rocks" Chambon, Desrues, Vardoulakis eds., Balkema, 59-72.

[13] di Prisco C, Matiotti R, Nova R. (1995). Theoretical investigation of the undrained stability of shallow submerged slopes, *Géotechnique* , **45**, 479-496.

[14] Ellison, K.C., Andrade, J.E. (2009). Liquefaction mapping in finite-element simulations. *J. Geotech. Geoenviron. Eng. ASCE*, Vol. 135, No. 11, 1693-1701.

[15] Hicks M. A., Boughrarou R. (1998). Finite element analysis of the Nerlerk underwater berm failures. *Géotechnique* 48, No. 2, 169–185.

[16] Hight D.W., Georgiannou V.N., Martin P.L. and Mundegar A.K. (1999) "Flow Slides in Micaceous Sands", *Proc. Int. Symp. On Problematic Soils*, Yanagisawa, E., Moroto, N. and Mitachi, T. eds., Balkema, Rotterdam, Sendai, Japan, pp. 945- 958.

[17] Imposimato S, Nova R. (1998). An investigation on the uniqueness of the incremental response of elastoplastic models for virgin sand, *Mechanics of Cohesive-Frictional Materials*, 3: 65-87.

[18] Ishihara, K. (1993). Liquefaction and flow failure during earthquakes. *Géotechnique* 43, No. 3, 351-415.

[19] Jefferies M.G.(1993). Nor**-**Sand**:** a simple critical state model for sand. *Géotechnique* 43, 91-103.

[20] Jefferies M.G.**,** Been K. (1991). Implications for critical state theory from isotropic compression of sand. *Géotechnique* 50:44, 419-429.

[21] Jefferies M.G. Been K. (2006). Soil Liquefaction: a critical state approach. Taylor and Francis Ed., New York.

[22] Klisinski M, Mroz Z, Runesson K. (1992). Structure of constitutive equations in plasticity for different choices of state and control variables. *International Journal of Plasticity*, 3, 221-243.

[23] Konrad J.M. (1991). The Nerlerk berm case history: some considerations for the design of hydraulic sand fills. *Can. Geotech. J.* 28(4): 601–612.

[24] Koppejan A.W., Wamelen B.M., Weinberg L.J.H (1948). Coastal flow slides in the Dutch province of Zeland. *Proc. II ICSMFE*, Rotterdam, Holland, Vol. 5, 89-96.

[25] Lade P. (1992). Static Instability and Liquefaction of Loose Fine Sandy Slopes. *Journal of Geotechnical Engineering*. Vol. 118, No. 1, pp. 51-71.

[26] Lade P. V. (1993). Initiation of static instability in the submarine Nerlerk berm. *Can. Geotech. J.* 30, 895-904.

[27] Maier, G., Hueckel, T., (1979). Non-associated and coupled flow-rules of elastoplasticity for rock-like materials. *Int. J. Rock. Mech. Min. Sci.* 16, 77-92.

[28] Mitchell, D.E. (1984). Liquefaction slides in hydraulically-placed sands. *Proc. 37th Can. Geotech. Conf.*,Ontario, pp. 141-146.

[29] Nova R. (1989). Liquefaction, stability, bifurcations of soil via strain-hardening plasticity. In E.Dembicki, G.Gudehus & Z. Sikora (eds) *Numerical Methods for Localisations and Bifurcations of granular bodies, Proc. Int. Works. Gdansk*, Technical Univeristy of Gdansk, 117-132.

[30] Nova, R. (1994). Controllability of the incremental response of soil specimens subjected to arbitrary loading programmes. *J. Mech. Behavior Mater.*, 5, No. 2, 193–201.

[31] Pestana J.M., Whittle A.J. (1995). Compression model for cohessionless soils, *Géotechnique*, 45 (4), 611-631.

[32] Pestana J.M., Whittle, A.J. (1999). Formulation of a unified constitutive model for clays and sands, *Int. J. Numer. Anal. Meth. Geomech.*, 23, 1215-1243.

[33] Pestana J.M., Whittle, A.J., Salvati L. (2002). Evaluation of a constitutive model for clays and sands: Part I Sand behavior, *Int. J. Numer. Anal. Meth. Geomech.*, 26, 1097-1121.

[34] Pestana, J.M., Nikolinakou, M.A., Whittle, A.J. (2005). Selection of material parameters for sands using the MIT-S1 model, *Proceedings of Geofrontiers 2005*, ASCE, Austin, TX.

[35] Pestana, J.M., Biscontin, G., Nadim, F., Andersen, K. (2000). Modeling cyclic behaviour of lightly overconsolidated clays in simple shear. *Soil Dynamics and Earthquake Engineering*; 19; 501-519.

[36] Pinheiro M., Wan, R.G. (2010). Finite element analysis of diffuse instability using an implicitly integrated pressure-density dependent elastoplastic model. *Finite Elements in Analysis and Design*, 46, 487-495.

[37] Poulos, S.J. (1981). The steady state of deformation. *Journal of the Geotechnical Engineering Division, ASCE.* 107(GT5): 553-562.

[38] Poulos, S.J., Castro, G. and France, J. (1985). Liquefaction evaluation procedure. *Journal of the Geotechnical Engineering Division, ASCE*. **111**(6): 772-792.

[39] Puzrin, A.M., Germanovich,L.N., Kim, S. (2004). Catastrophic failure of submerged slopes in normally consolidated sediments. *Géotechnique*, 54 (10), 631-643.

[40] Rogers, B. T., Been, K., Hardy, M. D., Johnson, G. J. & Hachey, J. E. (1990). Re-analysis of Nerlerk B-67 berm failures. *Proc. 43rd Can. Geotech. Conf.*, Quebec, pp. 227-237.

[41] Shibuya, S. (1985). Undrained behaviour of granular materials under principal stress rotation. PhD Thesis, University of London, 320 pp.

[42] Sladen, J. A., D'Hollander, R. D. & Krahn, J. (1985-a). The liquefaction of sands, a collapse surface approach. *Can. Geotech. J.* 22, 564-578.

[43] Sladen, J. A., D'Hollander, R. D., Krahn, J. & Mitchell D. E. (1985-b). Back analysis of the Nerlerk berm Liquefaction slides. *Can. Geotech. J.* 22, 579-588.

[44] Sladen J. A., D'Hollander, R. D., Krahn, J., Mitchell, D. E. (1987). Back analysis of the Nerlerk berm liquefaction slides: Reply. *Can. Geotech. J.* 24, 179-185.

[45] Terzaghi K. (1957). Varieties of submarine slope failures. *NGI Publication* N. 25, 1-16.

[46] Yoshimine, M., Robertson, P. K., (Fear) Wride, C.E. (1999). Undrained shear strength of clean sands to trigger flow liquefaction, *Can. Geotech. J.* 36(5): 891–906.

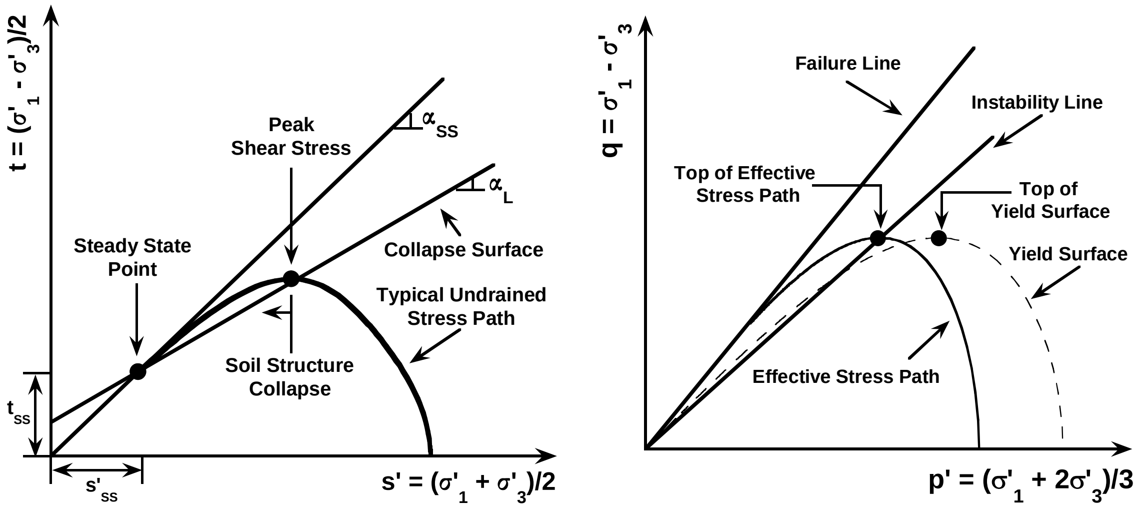

Fig. 1. a) Collapse Surface concept [redrawn after Sladen et al. 1985-a] ; b) Instability Line concept [redrawn after Lade 1992].

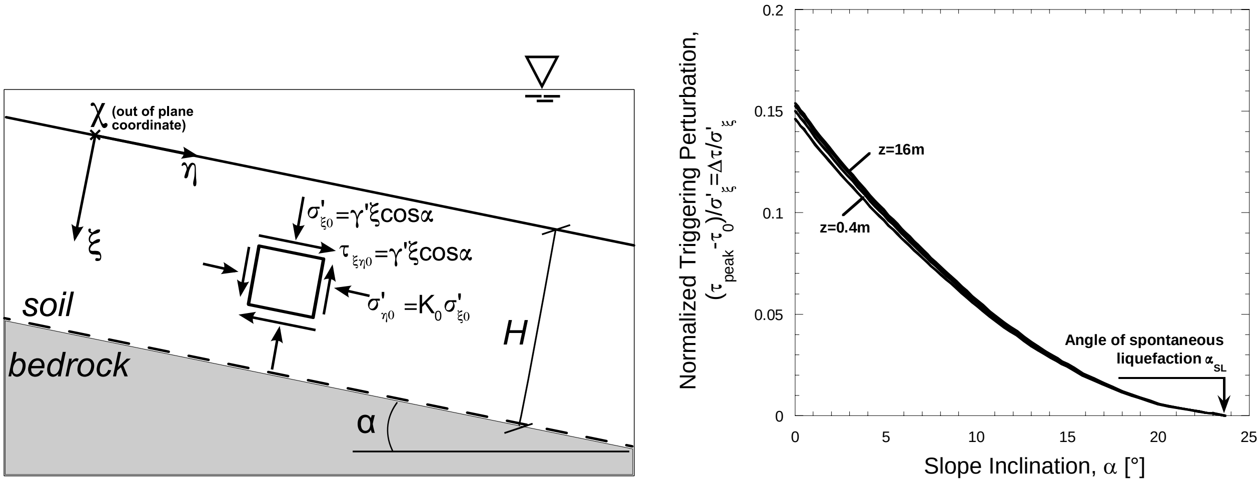

Figure 2. a) Reference system for a submerged infinite slope and initial stress conditions; b) Dependency of the triggering perturbation $\Delta\tau$ on the slope angle (results obtained with an elastoplastic soil model calibrated for loose Hostun sand; redrawn after di Prisco et al. (1995)).

Parameter / Symbol	Physical contribution / meaning	Toyura Sand	Nerlerk Sand 2% fines	Nerlerk Sand 12% fines
ρ_c	Compressibility of sands at large stresses (LCC regime)	0.37	0.44	0.44
p_{ref}/p_a	Reference stress at unit void ratio for conditions of hydrostatic compression in the LCC regime	55	65	65
θ	Describes first loading curve in the transitional stress regime	0.20	0.36	0.36
h	Irrecoverable plastic strains during reloading	-	-	-
K_{0NC}	K_0 in the LCC regime	0.49	0.50	0.50
μ'_0	Poisson's ratio at load reversal	0.23	0.23	0.23
ω	Non-linear Poisson's ratio. 1-D unloading stress path	1.00	1.00	1.00
ϕ'_{cs}	Critical state friction angle in triaxial compression	31.0°	31.0°	31.0°
ϕ'_{mr} p	Control the maximum friction angle as a function of formation density (at low effective stresses)	28.5° 2.45	25.0° 2.30	21.0° 2.60
m	Controls the cap geometry of the bounding surface	0.55	0.42	0.21
ω_s	Small strain (< 0.1%) non-linearity in shear	2.5	2.6	2.6
ψ	Rate of evolution of anisotropy. Stress-strain curves	50	30	30
C_b	Small strain stiffness at load reversal	750	400	400

Table I. Summary of MIT-S1 model parameters.

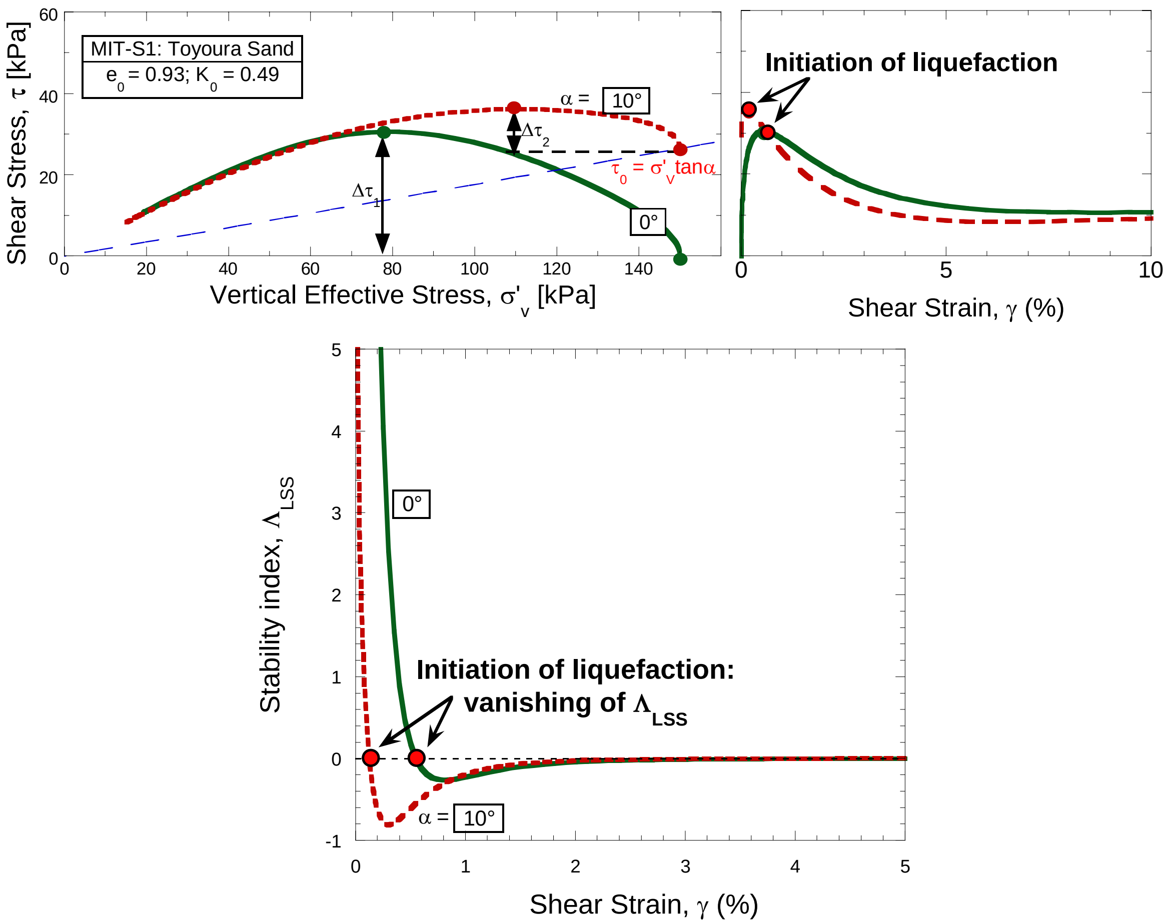

Figure 3. Example of simple shear simulations (loose Toyoura Sand):
a) stress path in the σ'_V-τ plane; b) stress strain behaviour;
c) evolution of the stability index Λ_{LSS} during the two simulations

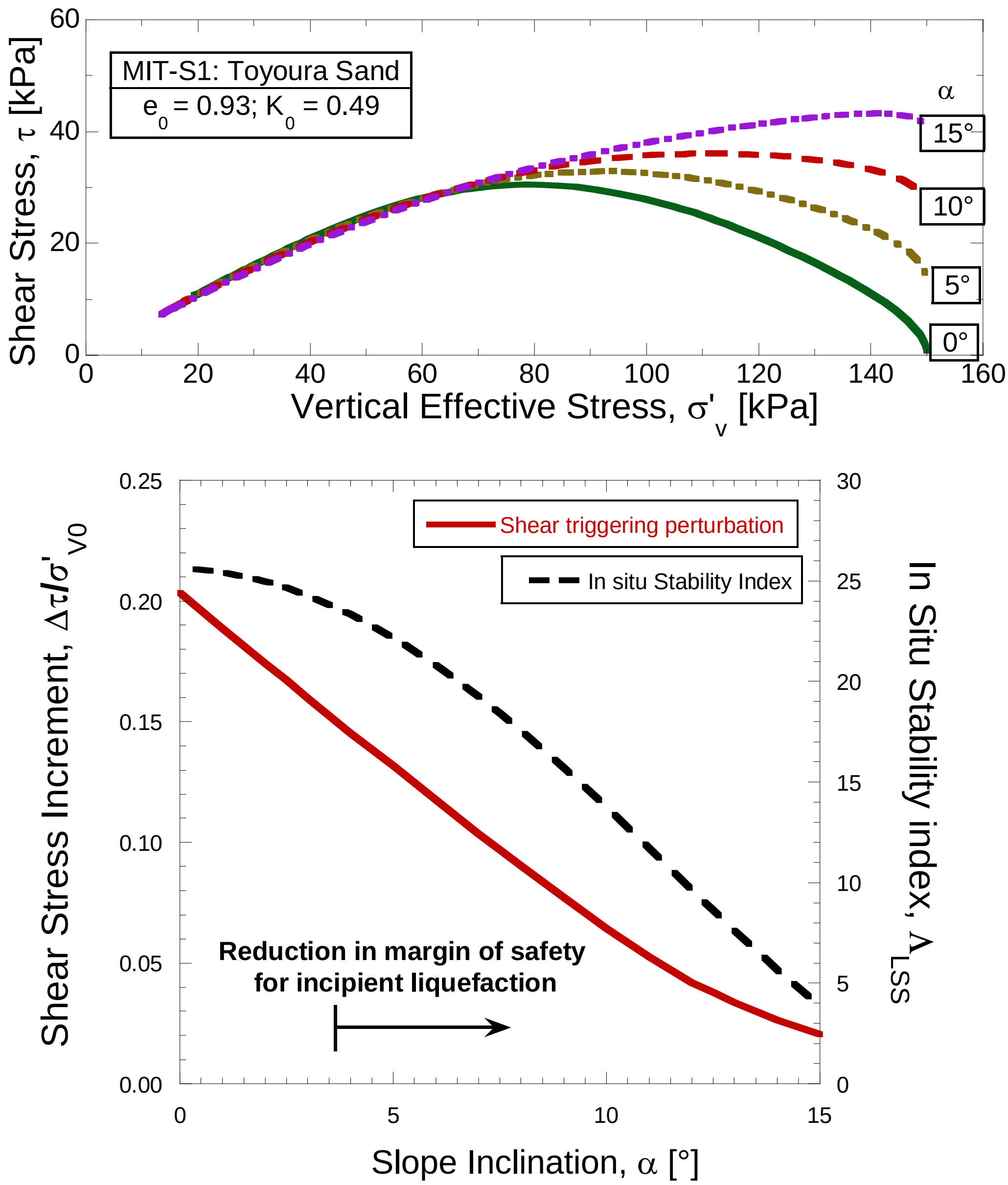

Figure 4. Effect of the slope angle: a) Stress path; b) Stability chart for an infinite slope made of loose Toyoura Sand and stability index Λ_{LSS} prior to undrained shearing as a function of the slope angle.

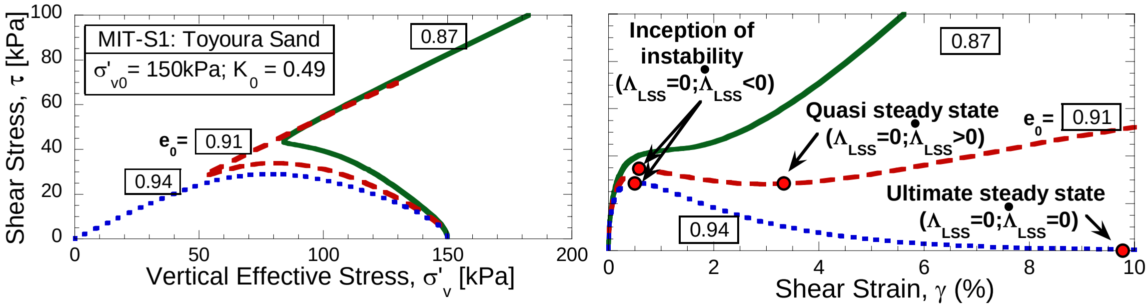

Figure 5. MIT-S1 predictions: effect of void ratio on undrained simple shear response of Toyoura Sand. a) stress path in the σ'$_V$-τ plane; b) stress-strain behaviour.

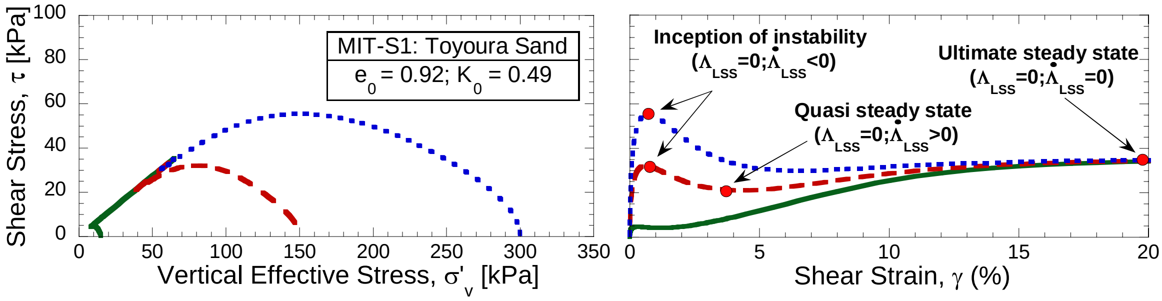

Figure 6. MIT-S1 predictions: effect of mean effective pressure on simple shear response of Toyoura Sand. a) stress path in the σ'_V-τ plane; stress-strain behaviour.

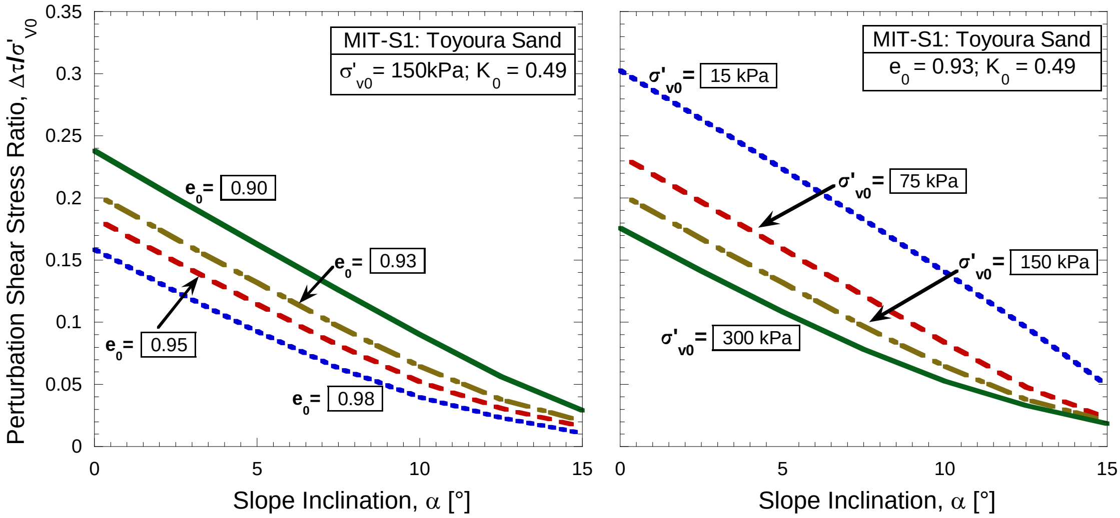

Figure 7. a) Effect of void ratio on stability charts for a given vertical effective stress; b) Effect of vertical effective stress on stability charts for a given void ratio.

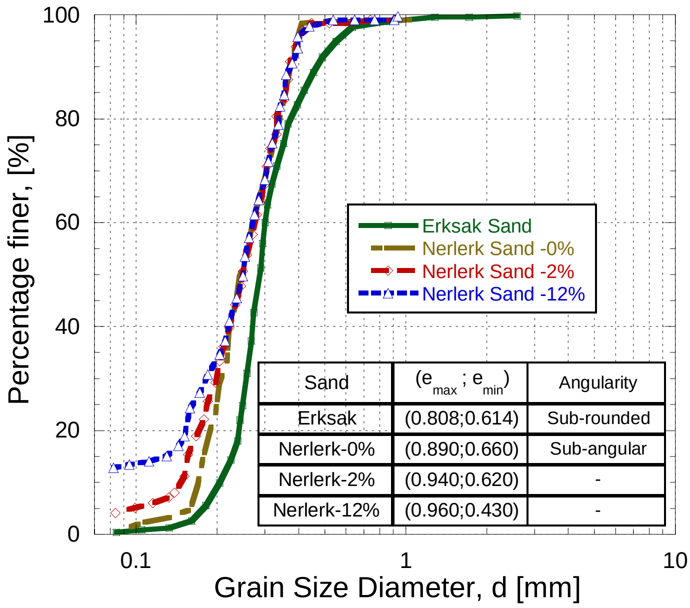

Figure 8. Grain size distribution curves for Erksak Sand and Nerlerk Sand at different fines percentages.

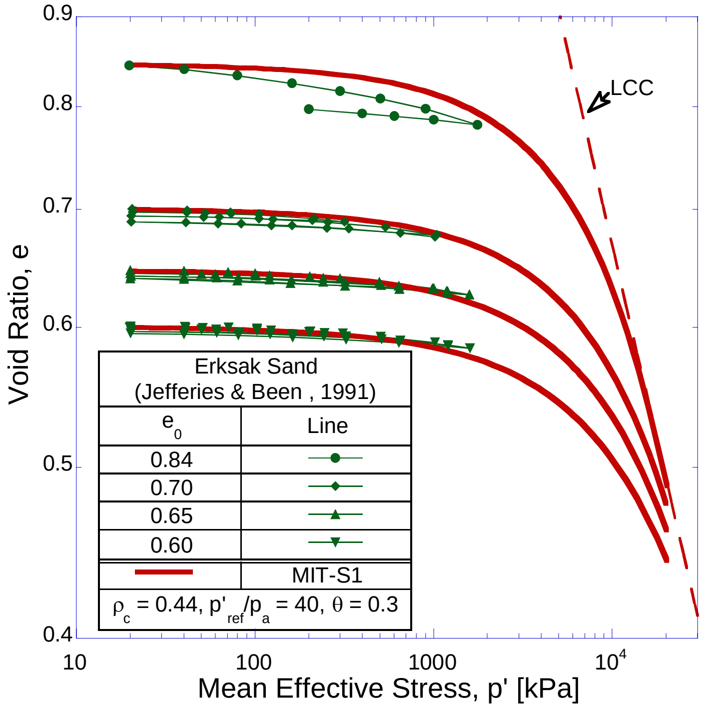

Figure 9. Simulation of Erksak sand compression behaviour: definition of the LCC curve.

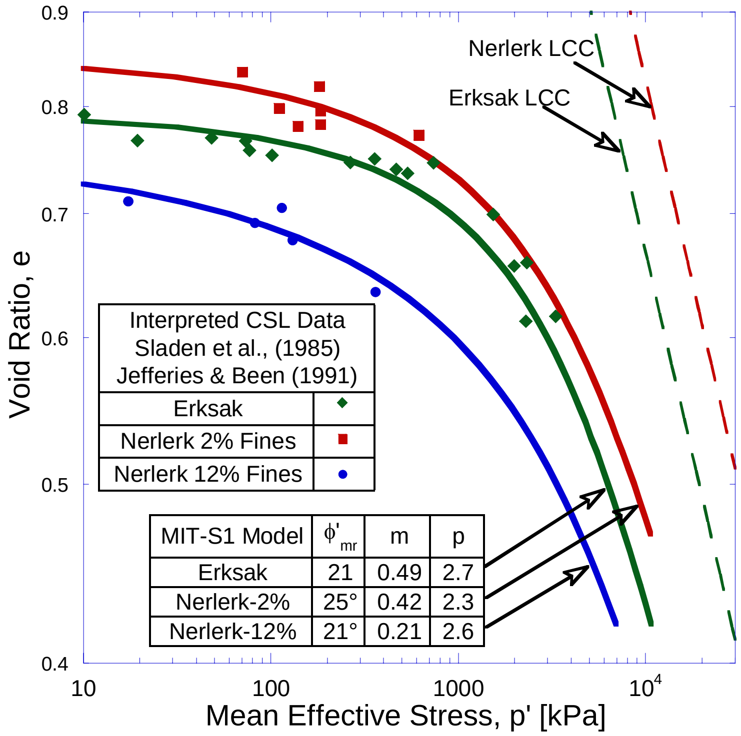

Figure 10. Comparison of CSL and LCC curves for Erksak sand and Nerlerk sand with 2% of fines

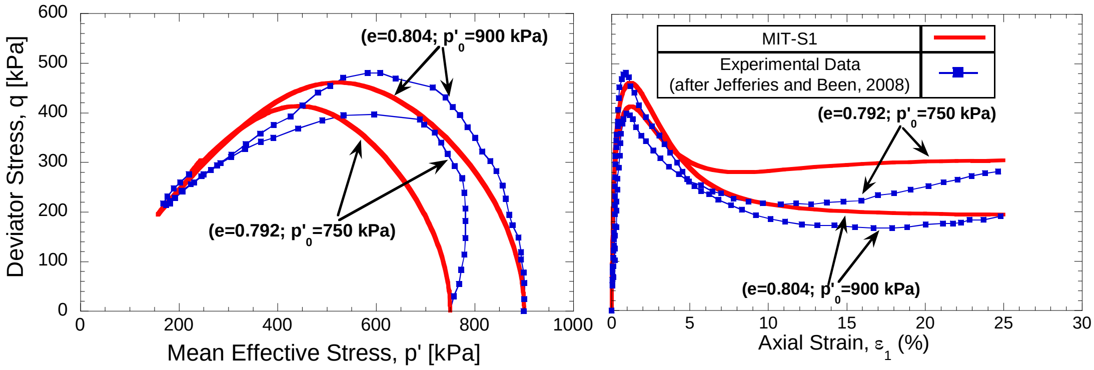

Figure 11. Calibration of undrained behaviour of Nerlerk Sand 2%: a) undrained stress paths; b) stress-strain response

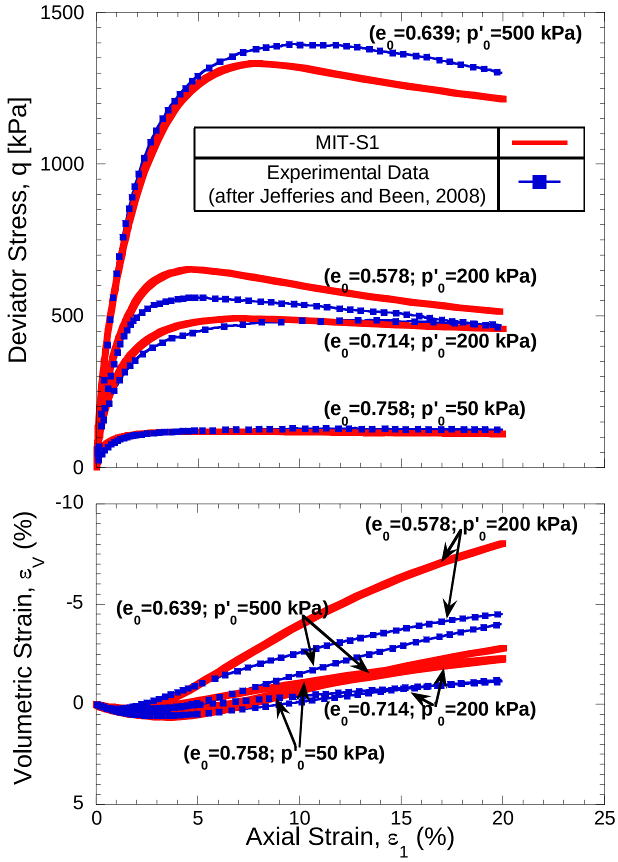

Figure 12. Calibration of the drained behaviour for Nerlerk Sand 2%: a) stress strain response; b) volumetric response

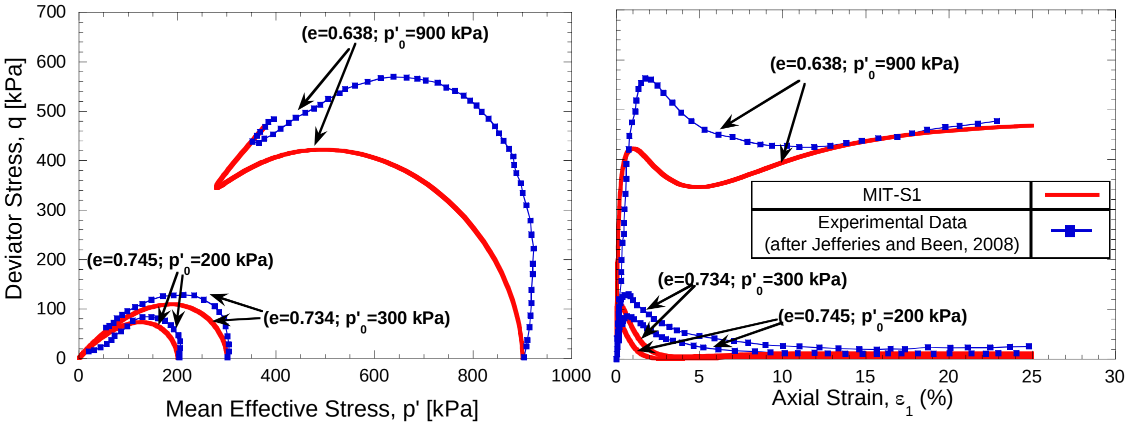

Figure 13. Comparison of computed and measured undrained shear behaviour for Nerlerk Sand 12%.

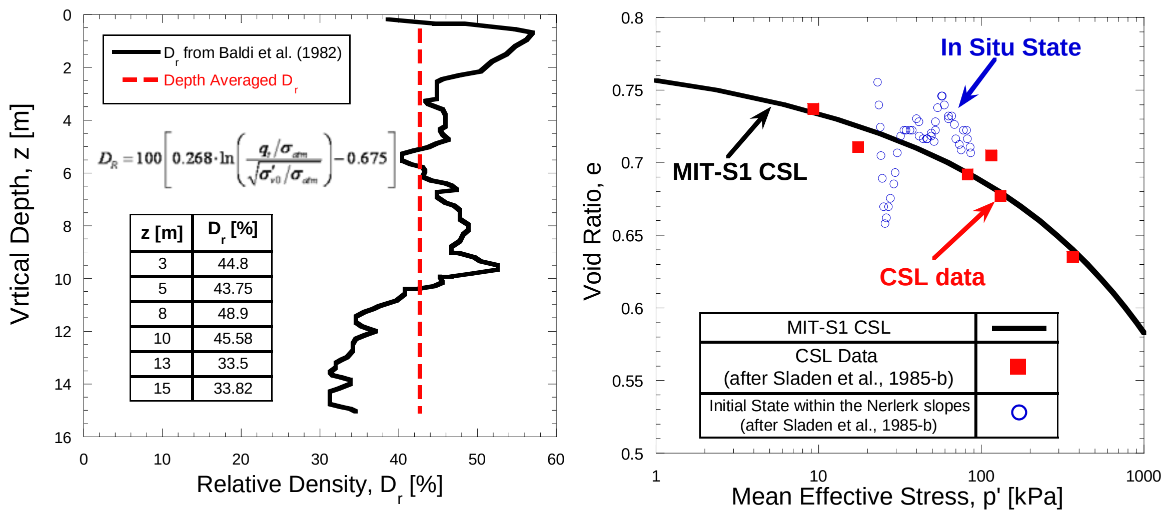

Figure 14. a) In situ relative density from CPT tests (Baldi et al. 1982); b) Location of in situ state on the CSL plane.

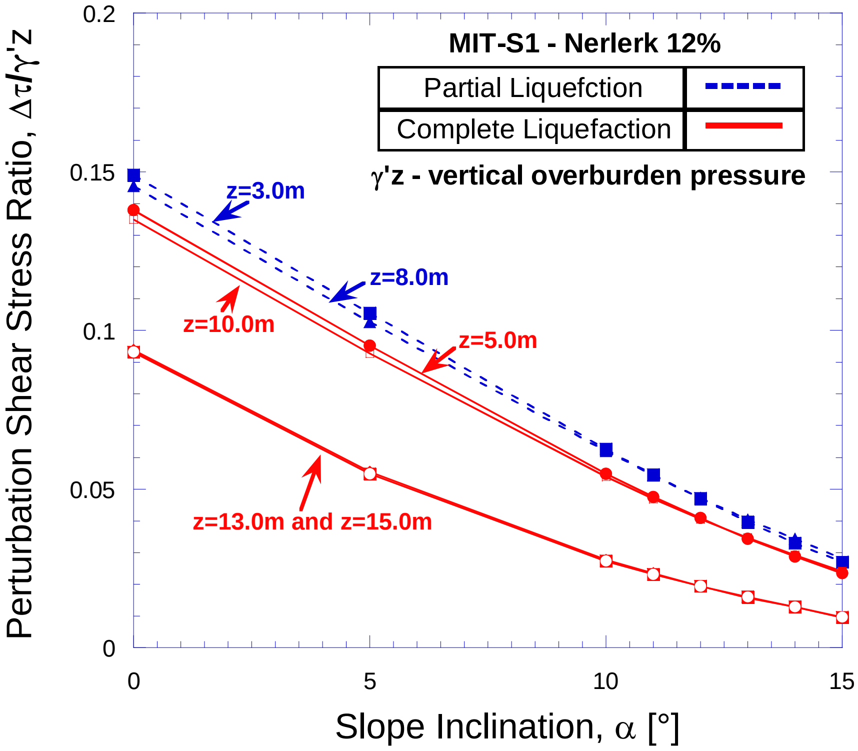

Figure 15. Stability charts for the Nerlerk berm.

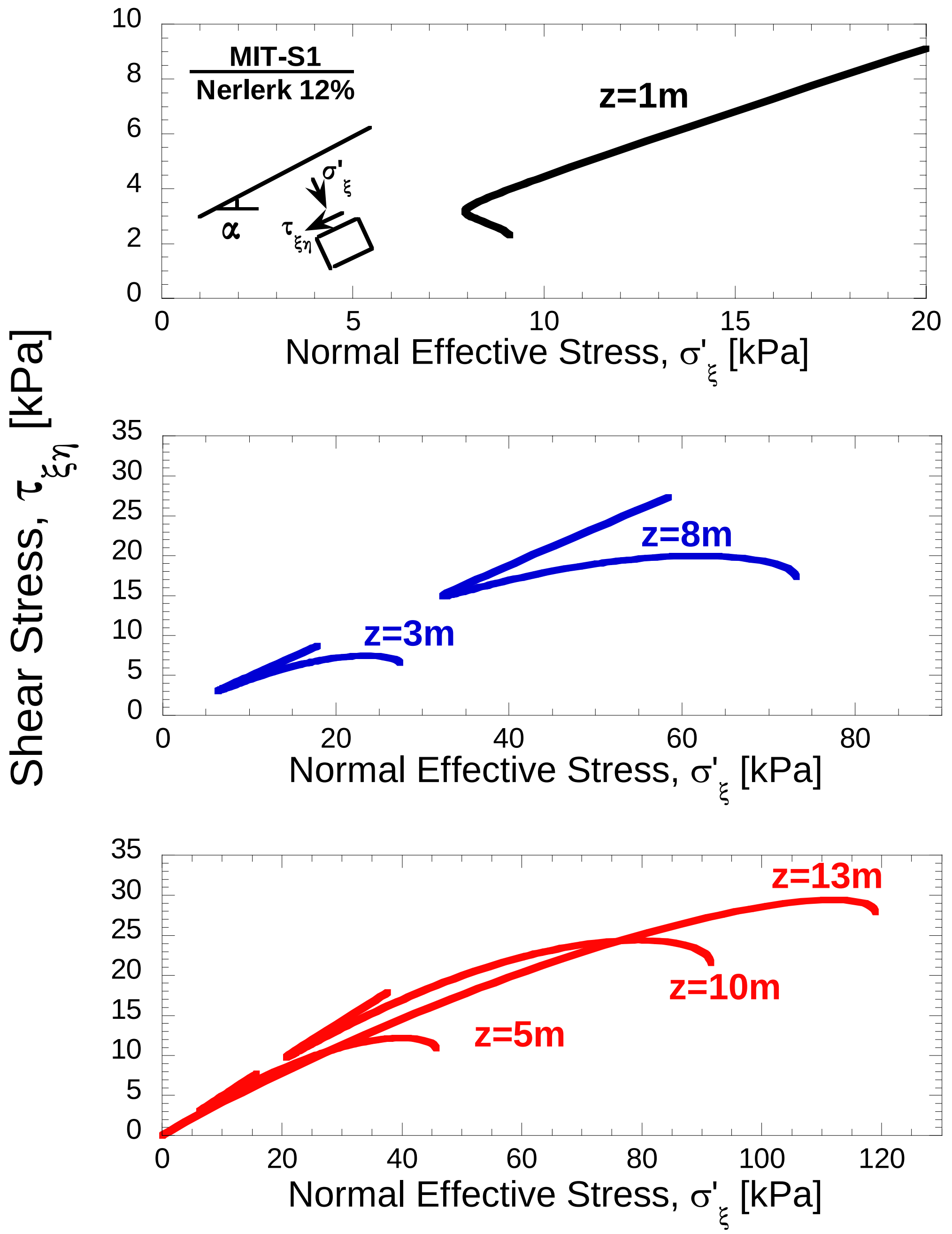

Figure 16. Example of undrained responses along the Nerlerk berm section (α=13°); a) No Liquefaction: b) Partial Liquefaction; c) Complete Liquefaction.

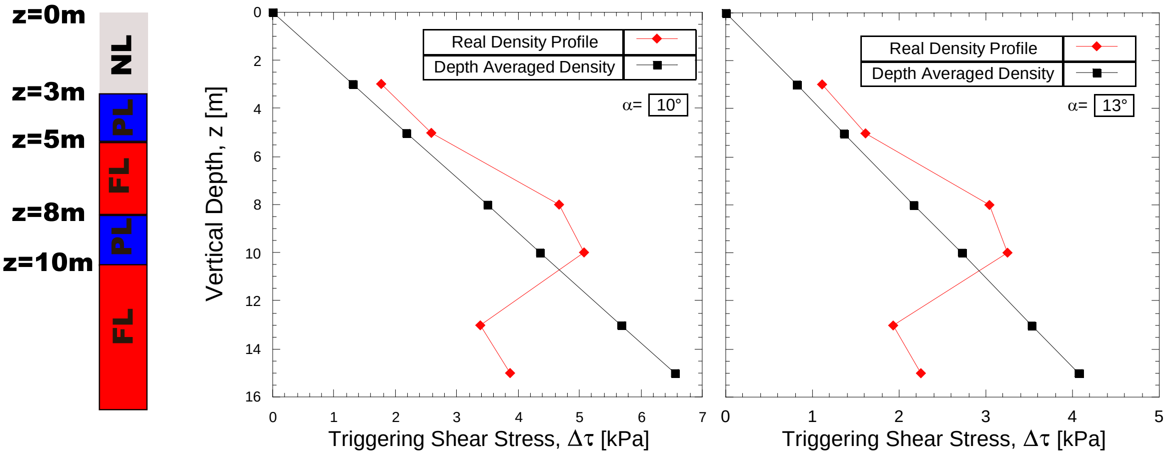

Figure 17. Variation with depth of undrained shear perturbation triggering liquefaction: a) Slope angle α=10°; b) Slope angle α=13° (NL stands for non liquefiable, PL for partial liquefaction and FL for full liquefaction).